



OPEN ACCESS

3-Hydroxybenzoate 6-Hydroxylase from *Rhodococcus jostii* RHA1 Contains a Phosphatidylinositol Cofactor

Edited by:

Daniela De Biase,
Sapienza Università di Roma, Italy

Reviewed by:

Hans-Peter Kohler,
Swiss Federal Institute of Aquatic
Science and Technology, Switzerland
Alberto A. Iglesias,
National University of the Littoral,
Argentina

***Correspondence:**

Willem J. H. van Berkel
willem.vanberkel@wur.nl

† Present address:

Stefania Montersino,
Adienne Pharma & Biotech, Milan,
Italy;
Evelien te Poele and Lubbert
Dijkhuizen,
CarbExplore Research BV, Groningen,
Netherlands;
Roberto Orru,
Institute of Molecular Biology,
Johannes Gutenberg University,
Mainz, Germany;
Robert van der Geize,
Laboratory of Pathology
East-Netherlands, Hengelo,
Netherlands
‡ These authors have contributed
equally to this work.

Specialty section:

This article was submitted to
Microbial Physiology and Metabolism,
a section of the journal
Frontiers in Microbiology

Received: 20 April 2017

Accepted: 31 May 2017

Published: 16 June 2017

Citation:

Montersino S, te Poele E, Orru R,
Westphal AH, Barendregt A,
Heck AJR, van der Geize R,
Dijkhuizen L, Mattevi A and
van Berkel WJH (2017)
3-Hydroxybenzoate 6-Hydroxylase
from *Rhodococcus jostii* RHA1
Contains a Phosphatidylinositol
Cofactor. *Front. Microbiol.* 8:1110.
doi: 10.3389/fmicb.2017.01110

Stefania Montersino^{1††}, Evelien te Poele^{2††}, Roberto Orru^{3†}, Adrie H. Westphal¹,
Arjan Barendregt⁴, Albert J. R. Heck⁴, Robert van der Geize^{2†}, Lubbert Dijkhuizen^{2†},
Andrea Mattevi³ and Willem J. H. van Berkel^{1*}

¹ Laboratory of Biochemistry, Wageningen University and Research, Wageningen, Netherlands, ² Microbial Physiology, Groningen Biomolecular Sciences and Biotechnology Institute, University of Groningen, Groningen, Netherlands,

³ Department of Biology and Biotechnology, University of Pavia, Pavia, Italy, ⁴ Biomolecular Mass Spectrometry and Proteomics, Bijvoet Center for Biomolecular Research and Utrecht Institute for Pharmaceutical Research, Utrecht University, Utrecht, Netherlands

3-Hydroxybenzoate 6-hydroxylase (3HB6H, EC 1.13.14.26) is a FAD-dependent monooxygenase involved in the catabolism of aromatic compounds in soil microorganisms. 3HB6H is unique among flavoprotein hydroxylases in that it harbors a phospholipid ligand. The purified protein obtained from expressing the gene encoding 3HB6H from *Rhodococcus jostii* RHA1 in the host *Escherichia coli* contains a mixture of phosphatidylglycerol and phosphatidylethanolamine, which are the major constituents of *E. coli*'s cytoplasmic membrane. Here, we purified 3HB6H (*Rj*3HB6H) produced in the host *R. jostii* RHA#2 by employing a newly developed actinomycete expression system. Biochemical and biophysical analysis revealed that *Rj*3HB6H possesses similar catalytic and structural features as 3HB6H, but now contains phosphatidylinositol, which is a specific constituent of actinomycete membranes. Native mass spectrometry suggests that the lipid cofactor stabilizes monomer-monomer contact. Lipid analysis of 3HB6H from *Pseudomonas alcaligenes* NCIMB 9867 (*Pa*3HB6H) produced in *E. coli* supports the conclusion that 3HB6H enzymes have an intrinsic ability to bind phospholipids with different specificity, reflecting the membrane composition of their bacterial host.

Keywords: expression strain, flavoprotein, monooxygenase, phospholipid, *Rhodococcus*

INTRODUCTION

Rhodococcus jostii RHA1 is a biotechnologically and environmentally important bacterium from the order Actinomycetales. Together with the genera *Nocardia*, *Corynebacterium* and *Mycobacterium*, *Rhodococcus* forms a distinct group of bacteria called mycolata (Finnerty, 1992; Brennan and Nikaido, 1995; Chun et al., 1996; Gürtler et al., 2004), characterized by a complex

Abbreviations: 3HB6H, recombinant 3-hydroxybenzoate 6-hydroxylase from *Rhodococcus jostii* RHA1 produced in *Escherichia coli*; *Pa*3HB6H, recombinant 3-hydroxybenzoate 6-hydroxylase from *Pseudomonas alcaligenes* NCIMB 9867 produced in *Escherichia coli*; PE, phosphatidylethanolamine; PG, phosphatidylglycerol; PI, phosphatidylinositol; *Rj*3HB6H, recombinant 3-hydroxybenzoate 6-hydroxylase from *Rhodococcus jostii* RHA1 produced in *Rhodococcus jostii* RHA1#2.

cell envelope (Sutcliffe, 1998; Guerin et al., 2010; De Carvalho et al., 2014) and an impressive catabolic diversity, allowing adaptation to different carbon sources for growth (van der Geize and Dijkhuizen, 2004). In comparison with other mycolata, *R. jostii* RHA1 is particularly rich in oxygenases (203 putative genes) and ligases (192 putative genes), gained primarily through ancient gene duplications or acquisitions (McLeod et al., 2006; Yam et al., 2010).

We recently reported the crystal structure of *R. jostii* RHA1 3-hydroxybenzoate 6-hydroxylase (3HB6H), produced as a recombinant protein in *Escherichia coli* (Montersino et al., 2013). 3HB6H (EC 1.13.14.26) is a NADH and FAD-dependent monooxygenase that catalyzes the *para*-hydroxylation of 3-hydroxybenzoate to 2,5-dihydroxybenzoate, using a Tyr-His pair for substrate binding and catalysis (Sucharitakul et al., 2015). The crystal structure analysis revealed that 3HB6H has the conserved fold of group A flavoprotein hydroxylases (Montersino et al., 2011; Huijbers et al., 2014), but differs from the other family members in additional binding of phospholipids. The tightly bound phospholipids were identified as a mixture of PG and PE, which are the major constituents of the *E. coli* cytoplasmic membrane (Pulfer and Murphy, 2003; Oursel et al., 2007). The fatty acyl chains of the phospholipid ligands of 3HB6H protrude into the substrate-binding pockets, whereas the surface-exposed hydrophilic headgroups are involved in enzyme dimerization (Figure 1) (Montersino et al., 2013).

To shed more light on the role of these lipid guests, bearing in mind the different lipid compositions of Gram-positive and Gram-negative bacterial membranes (Finnerty, 1992; Sutcliffe, 1998), in the present work we produced *Rj3HB6H* in a newly developed *R. jostii* RHA1#2 expression strain and, in addition, 3HB6H from *Pseudomonas alcaligenes* NCIMB 9867 (*Pa3HB6H*) in *E. coli*. Biochemical and biophysical characterization revealed that *Rj3HB6H* possesses similar catalytic and structural features as 3HB6H, but contains PI as glycerophospholipid ligand. Lipid analysis of *Pa3HB6H* indicates that lipid binding is an intrinsic property of prokaryotic 3-hydroxybenzoate 6-hydroxylases.

MATERIALS AND METHODS

Chemicals

Aromatic compounds were purchased from Sigma-Aldrich (St Louis, MO, United States) and Acros Organics (Morris Plains, NJ, United States). Catalase, FAD, FMN, arabinose, antibiotics, Terrific broth (TB) and LB broth (Miller) (LB) were from Sigma-Aldrich (St Louis, MO, United States). Pefabloc SC and DNase I were obtained from Roche Diagnostics GmbH (Mannheim, Germany). Restriction enzymes and *Pfu* DNA polymerase were from Thermo Fischer Scientific (United States). 4-androstene-3,17-dione was from Merck (Oss, Netherlands). Crystallization kits were purchased from New Hampton (Aliso Viejo, CA, United States). Immobilized metal affinity chromatography columns (His GraviTrap) were from GE Healthcare Bioscience AB (Uppsala, Sweden). All other chemicals were from commercial sources and of the purest grade available.

Bacterial Strains and Primers

All bacterial strains and primers used in this study are listed in Tables 1, 2.

Construction of *Rhodococcus* Expression Vector Q2+

The *E. coli*-*Rhodococcus* shuttle vector pRESQ (van der Geize et al., 2002) was modified by insertion of the RP4 *oriT* of pK18*mobsacB* (Schäfer et al., 1994) enabling trans-conjugal transfer of the resulting vector. For this, the *oriT*-region was amplified from pK18*mobsacB* by PCR using forward primer *oriT*-F and reverse primer *oriT*-R (Table 1). The obtained 549 bp PCR-product was cloned into the *Sma*I-site of pRESQ, resulting in pQmob. A duplicate region of 424 bp on pQmob was removed by deleting the 760 bp *Xba*I-*Bsp*HI fragment, yielding pQmobΔd. The *egfp* gene from pIJ8630 (Sun et al., 1999) was amplified by PCR using forward primer *egfp*-*Pci*I-F, containing a *Pci*I restriction site, and reverse primer *egfp*-*Pci*I-R, also containing a *Pci*I restriction site (Table 1). The 744 bp *Pci*I-*Pci*I fragment containing the *egfp* gene was cloned into the *Pci*I-site of pQmobΔd to generate peGFPQ.

The *R. jostii* strain RHA1 genomic region consisting of gene *ro00440*, its promoter region and the *prmA* promoter (*PprmA*) (here referred to as region *reg1*-*PprmA*; GenBank accession number CP000431: nt 521345 - nt 523358) was amplified from genomic DNA of *R. jostii* RHA1 by PCR using forward primer *reg1*-*Bgl*II-F, containing a *Bgl*II restriction site, and reverse primer *prmA*-*Nde*I-R, containing an *Nde*I restriction site (Table 1). The 2014 bp *Bgl*II-*Nde*I *reg1*-*PprmA* fragment was cloned into the *Bgl*II-*Nde*I sites of peGFPQ, yielding prMOeGFPQ1.

The *R. jostii* RHA1 gene *ro00452* and its promoter region (here referred to as region *reg2*; CP000431: nt 534363 - nt 536227) were amplified by PCR using forward primer *reg2*-*Pci*I-F, containing a *Pci*I restriction site and reverse primer *reg2*-*Pci*I-R, also containing a *Pci*I restriction site (Table 1). The 1880 bp *Pci*I-*Pci*I *reg2* fragment was cloned into the *Pci*I-site of prMOeGFPQ1, resulting in prMOeGFPQ2.

For construction of expression vector Q2+, the *egfp* gene of prMOeGFPQ2 was replaced with a multiple cloning site (MCS). For this, part of the MCS of pBluescript KS was amplified by PCR using forward primer MCS-*Nde*I-F, containing an *Nde*I restriction site and reverse primer MCS-*Pci*I-R, containing a *Pci*I restriction site (Table 1). The 125 bp *Nde*I-*Pci*I MCS fragment was cloned into the *Nde*I-*Pci*I site of prMOeGFPQ2, replacing the *Nde*I-*Pci*I region containing *egfp*, resulting in the expression vector Q2+.

Cloning and Production of 3HB6H in *R. jostii* RHA1#2

The 1321 bp *Nde*I-*Xmn*I fragment of pBAD-3HB6H-His₆ (Montersino and van Berkel, 2012) containing the 3HB6H gene including the His₆-tag, was cloned into the *Nde*I-*Hind*III (Klenow-fragment treated) site of expression vector Q2+ to generate Q2+-3HB6H-His₆.

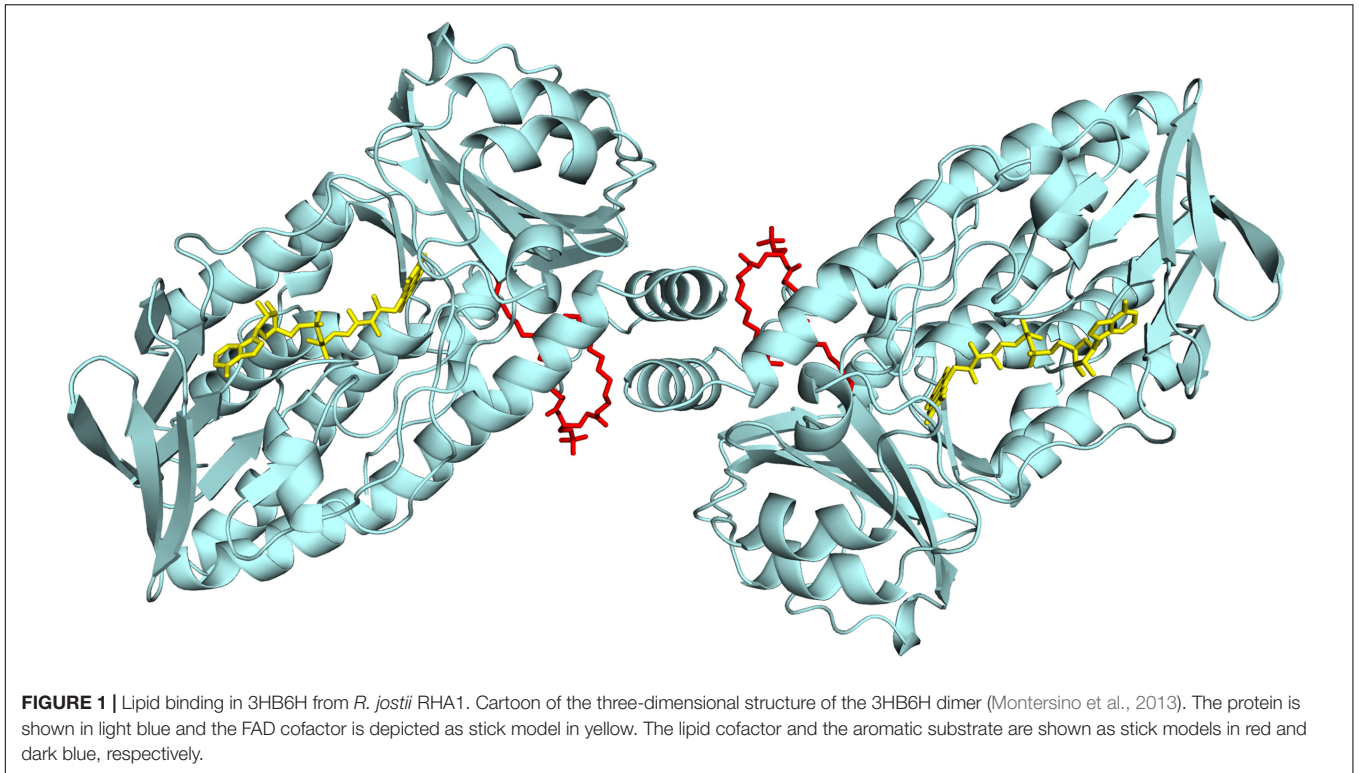


TABLE 1 | List of primers used in PCR.

| | |
|----------------------|--|
| <i>oriT</i> -F | 5'-CATAGTCCACGACGCC-3' |
| <i>oriT</i> -R | 5'-TCTTTGGCATCGTCTCTCG-3' |
| <i>egfp-Pcil</i> -F | 5'-GCACATGTCGGAGGTCCATATGGCCATGGT-3' |
| <i>egfp-Pcil</i> -R | 5'-GCACATGTATTACTTGTACAGCTCGTCCATGC-3' |
| <i>reg1-BglII</i> -F | 5'-GGAGATCTGACATCCCGCGATACG-3' |
| <i>prmA-NdeI</i> -R | 5'-GGCATATGTGCGCCTCCTGGATCG-3' |
| <i>reg2-Pcil</i> -F | 5'-GGACATGTCCGGTCTCCACCACCCCGTCT-3' |
| <i>reg2-Pcil</i> -R | 5'-GGACATGTCCGGTCTCCACCACCCCGTCT-3' |
| MCS- <i>NdeI</i> -F | 5'-TTGCATATGCACCGCGGTGGC-3' |
| MCS- <i>Pcil</i> -R | 5'-GGGAACATGTGCTGGGTACC-3' |

TABLE 2 | List of bacterial strains.

| | |
|--------------------------------|---|
| <i>R. jostii</i> RHA1 | The complete genome of <i>Rhodococcus</i> sp. RHA1 provides insights into a catabolic powerhouse. (McLeod et al., 2006) |
| <i>R. jostii</i> strain RHA1#2 | Used as a host for protein production. This strain is a spontaneous mutant of <i>R. jostii</i> RHA1, carrying deletions of ~0.9 Mb on the 1.12 Mb linear plasmid pRHL1 and ~0.2 Mb on the 0.44 Mb linear plasmid pRHL2. The deletions together comprise ~11.3% of the 9.7 Mb <i>R. jostii</i> genome. |
| <i>E. coli</i> DH5 α | Used as host for cloning procedures. |
| <i>E. coli</i> TOP10 | Used for production of 3HB6H (Montersino and van Berkel, 2012) and <i>Pa</i> 3HB6H. |

Rhodococcus cells were electroporated as described previously (van der Geize et al., 2000). Prior to electroporation, plasmid DNA was desalted by dialyzing 10 μ L plasmid DNA for 30 min

on a Millipore “V” Series filter disk (0.025 μ m) floating on MiliQ water.

Cultures of *R. jostii* RHA1#2 were grown in LB broth supplemented with 50 μ g·mL⁻¹ kanamycin at 30°C at 200 rpm. *R. jostii* RHA1#2 cells harboring Q2+3HB6H-His₆ were grown overnight in 3 mL LB broth, diluted 1:300 in 300 mL LB broth in a 3 L Erlenmeyer flask and grown for 20–24 h. Cultures were induced by adding 2 mM 4-androstene-3,17-dione dissolved in acetone. Growth was continued for 48 h after induction. Cells were harvested by centrifugation at 4°C and pellets were washed once with ice-cold 20 mM potassium phosphate, pH 7.2, containing 300 mM NaCl. After centrifugation at 4°C, cells were stored at -20°C.

Cloning and Production of 3HB6H from *Pseudomonas alcaligenes* NCIMB 9867

The *xlnD* gene sequence encoding for *Pa*3HB6H (UniProt: Q9F131) was synthesized and subcloned in a pBAD vector by GeneArt (Invitrogen, Carlsbad, CA, United States). The resulting construct (pBAD-*Pa*3HB6H-His₆) was verified by automated sequencing of both strands and electroporated into *E. coli* TOP10 cells for recombinant expression.

For enzyme production, *E. coli* TOP10 cells, harboring the pBAD-*Pa*3HB6H-His₆ plasmid, were grown in TB medium at 37°C supplemented with 100 μ g·mL⁻¹ ampicillin until an optical density (OD_{600 nm}) of 0.8 was reached. Expression was induced by the addition of 0.02% (w/v) arabinose and incubation was continued for 40 h at 17°C. Cells were harvested by centrifugation at 4°C and stored at -20°C.

Enzyme Purification

Rj3HB6H was purified to apparent homogeneity using an Äkta Explorer chromatography system (GE-Healthcare). *R. jostii* RHA1#2 cells containing the recombinant protein were suspended in ice-cold 20 mM potassium phosphate, pH 7.2, containing 300 mM NaCl, 1 mM Pefabloc SC, 1 mg DNase and 100 μM MgCl_2 , and subsequently passed twice through a precooled French Pressure cell (SLM Aminco, SLM Instruments, Urbana, IL, United States) at 16,000 psi. The resulting homogenate was centrifuged at $25,000 \times g$ for 45 min at 4°C to remove cell debris, and the supernatant was applied onto a Ni-NTA agarose column (16 mm \times 50 mm) equilibrated with 20 mM potassium phosphate, pH 7.2, containing 300 mM NaCl. After washing with five volumes of equilibration buffer, the enzyme was eluted with 300 mM imidazole in equilibration buffer. The resulting *Rj3HB6H* fraction was supplemented with 100 μM FAD and loaded onto a Source Q-15 anion exchange column (16 mm \times 90 mm), pre-equilibrated with 50 mM Bis-Tris, 0.1 mM EDTA, pH 7.2. After washing with two volumes of equilibrating buffer, the enzyme was eluted with a linear gradient of 0–1 M NaCl in the same buffer. Active fractions were pooled, concentrated to 10 $\text{mg}\cdot\text{mL}^{-1}$ using ultrafiltration (Amicon 30 kDa cutoff filter), and applied onto a Superdex S-200 (26 mm \times 600 mm) column running in 50 mM potassium phosphate, 150 mM NaCl, pH 7.2. Active fractions were concentrated to 10 $\text{mg}\cdot\text{mL}^{-1}$ using ultrafiltration (Amicon 30 kDa cutoff filter) and dialyzed at 4°C against 50 mM Bis-Tris, pH 7.2. The final *Rj3HB6H* preparation showed a single band after SDS-PAGE. The specific activity of the purified enzyme was 21 $\text{U}\cdot\text{mg}^{-1}$ using the standard activity assay (Table 3A).

Pa3HB6H was purified to apparent homogeneity, applying essentially the same procedure as described above for *Rj3HB6H*. The final *Pa3HB6H* preparation showed a single band after SDS-PAGE. The specific activity of the purified enzyme was 34 $\text{U}\cdot\text{mg}^{-1}$ using the standard activity assay (Table 3B).

Purified enzymes were flash frozen in 1 mL aliquots in liquid nitrogen and stored at -80°C . Before use, thawed enzyme samples were incubated with 0.1 mM FAD and excess FAD was removed using a gel filtration column (10 mm \times 100 mm) containing Bio-Gel P-6DG.

Biochemical Characterization

Molar absorption coefficients of protein-bound FAD were determined from absorption spectra of *Rj3HB6H* and *Pa3HB6H* recorded in the presence and absence of 0.1% (w/v) SDS, assuming a molar absorption coefficient for free FAD of $11.3\text{ mM}^{-1}\cdot\text{cm}^{-1}$ at 450 nm. The enzyme concentration of *Rj3HB6H* was determined by measuring the absorbance at 453 nm using a molar absorption coefficient for protein-bound FAD of $10.3\text{ mM}^{-1}\cdot\text{cm}^{-1}$. The enzyme concentration of *Pa3HB6H* was determined by measuring the absorbance at 450 nm using a molar absorption coefficient for protein-bound FAD of $11.0\text{ mM}^{-1}\cdot\text{cm}^{-1}$. *Rj3HB6H* and *Pa3HB6H* activity was determined at 25°C by measuring NADH consumption at 360 nm (Montersino and van Berkel, 2012). The standard assay mixture contained 50 mM Tris- SO_4 , pH 8.0, 200 μM

4-hydroxybenzoate and 250 μM NADH. Steady-state kinetic parameters were determined from measurements at 25°C in 50 mM Tris- SO_4 , pH 8.0. Hydroxylation efficiencies were determined by oxygen consumption experiments, essentially as described before (Montersino and van Berkel, 2012).

Crystallization and Structure Determination

Crystals of *Rj3HB6H* for structure determination were obtained by the sitting drop vapor diffusion method at 20°C by mixing equal volumes (2 μL) of protein and reservoir solutions. Protein solutions consisted of 30 $\text{mg}\cdot\text{mL}^{-1}$ enzyme in 1 mM FAD, 2 mM 3-hydroxybenzoate, and 50 mM Bis-Tris, pH 7.2, whereas precipitant solutions consisted of 30% PEG 4000, 0.2 M lithium sulfate, and 0.1 M Tris-HCl, pH 8.5. Yellow crystals grew in 1 day.

X-ray diffraction data were collected at Grenoble and processed with the CCP4 package (Winn et al., 2011). The *Rj3HB6H* structure was solved by molecular replacement using the structure of a monomer of 3HB6H (pdb entry: 4BJZ) as search model. Crystallographic computing and model analysis were performed with COOT (Emsley et al., 2010), PHENIX (Adams et al., 2010) and the CCP4 package (Potterton et al., 2004). Pictures were generated with Pymol (Schrodinger, 2015) and CCP4 (Potterton et al., 2004). Data collection parameters and refinement statistics are presented in Table 4.

The atomic coordinates and structure factors of *Rj3HB6H* (code 5HYM) have been deposited in the Protein Data Bank¹.

Lipid Identification and Native ESI-MS Experiments

Extraction and identification of protein-bound lipids from *Rj3HB6H* and *Pa3HB6H* was performed as described for 3HB6H (Montersino et al., 2013). For nanoflow ESI-MS analysis under native conditions, enzyme samples were prepared in 50 mM ammonium acetate, pH 6.8. For analysis under denaturing conditions, enzyme samples were diluted either in 50% acetonitrile with 0.2% formic acid or in 5% formic acid. Native MS analysis was performed using a LC-T nanoflow ESI orthogonal TOF mass spectrometer (Micromass, Manchester, United Kingdom) in positive ion mode with a capillary voltage of 1.3 kV. The cone voltage was varied between 90 and 150 V and source pressure was set to 6.9 mbar to enhance transmission of large ions. Lipid identification was performed using a Quattro Ultima nanoflow triple quadrupole mass spectrometer (Micromass, Manchester, United Kingdom) in negative ion mode, with a capillary voltage of 1.3 kV and a cone voltage of 150 V. For MS/MS analysis, argon was supplied in the collision cell (2.0×10^{-3} bar). Collision energy was adjusted to gain optimal fragmentation. Both mass spectrometers were equipped with a Z-spray nano-electrospray ionization source. Measurements were performed by using gold-coated needles, made from borosilicate glass capillaries (Kwik-Fill; World precision Instruments, Sarasota) on a P-97 puller (from Sutter Instruments, Novato, CA, United States). Needles were coated

¹<http://pdbe.org/5HYM>

with a gold layer using an Edwards Scancoat six Pirani 501 sputter coater (Edwards laboratories, Milpitas, CA, United States). All TOF spectra were mass calibrated by using an aqueous solution of cesium iodide (25 mg·mL⁻¹).

Sequence Comparison

Protein sequences were retrieved using protein resources from the National Centre for Biotechnology Information² and UniProt Database³. Multiple sequence alignments were made using CLUSTALW (Thompson et al., 1994). Phylogenetic plots were made using FigTree⁴.

RESULTS

Biochemical Properties of *Rj3HB6H*

Expression of the 3HB6H gene from *R. jostii* RHA1#2 yielded about 7 mg of purified *Rj3HB6H* protein from 10 g wet cells (Table 3A). *Rj3HB6H* displayed the same absorption spectrum as 3HB6H, with maxima at 274, 383, and 453 nm and a shoulder at 480 nm (Montersino and van Berkel, 2012). A molar absorption coefficient of protein-bound flavin, $\epsilon_{453} = 10.3 \text{ mM}^{-1} \text{ cm}^{-1}$, was used for both proteins.

Determination of steady-state kinetic parameters revealed that *Rj3HB6H* behaves similarly as 3HB6H using 3-hydroxybenzoate as variable substrate and fixed NADH concentration ($k_{\text{cat}} = (20 \pm 1) \text{ s}^{-1}$; $K_{\text{M}} = (35 \pm 3) \mu\text{M}$; $k_{\text{cat}}/K_{\text{M}} = (5.7 \pm 0.8) \times 10^5 \text{ s}^{-1} \cdot \text{M}^{-1}$) and with variable concentration of NADH (preferred coenzyme) and fixed 3-hydroxybenzoate concentration ($k_{\text{cat}} = (20 \pm 1) \text{ s}^{-1}$; $K_{\text{M}} = (68 \pm 5) \mu\text{M}$; $k_{\text{cat}}/K_{\text{M}} = (3.0 \pm 0.4) \times 10^5 \text{ s}^{-1} \cdot \text{M}^{-1}$). *Rj3HB6H* displays a very low NADH oxidase activity (<1 U·mg⁻¹). Uncoupling of hydroxylation of 3-hydroxybenzoate occurs to a minor extent (less than 10%), while 2,5-dihydroxybenzoate is a strong non-substrate effector ($k_{\text{cat}} = (6 \pm 0.8) \text{ s}^{-1}$; $K_{\text{M}} = (150 \pm 30) \mu\text{M}$; $k_{\text{cat}}/K_{\text{M}} = (4.0 \pm 1.3) \times 10^4 \text{ s}^{-1} \cdot \text{M}^{-1}$), efficiently stimulating the rate of flavin reduction by NADH (Montersino and van Berkel, 2012; Sucharitakul et al., 2012, 2013; Ni et al., 2016).

Structural Characterization

Rj3HB6H crystals grew in similar conditions as found for 3HB6H, and are isomorphous to those of 3HB6H, where

²www.ncbi.nlm.nih.gov

³http://www.uniprot.org/www.uniprot.org

⁴tree.bio.ed.ac.uk

TABLE 3A | Purification of *Rj3HB6H* produced in *R. jostii* RHA1#2.

| Step | Protein (mg) | Activity (U) | Specific activity (U·mg ⁻¹) | Yield (%) |
|---------------|--------------|--------------|---|-----------|
| Cell extract | 208 | 355 | 2 | 100 |
| His GraviTrap | 37 | 300 | 8 | 84 |
| Mono-Q | 16 | 230 | 14 | 65 |
| His GraviTrap | 7 | 168 | 21 | 47 |

TABLE 3B | Purification of *Pa3HB6H* produced in *E. coli*.

| Step | Protein (mg) | Activity (U) | Specific activity (U·mg ⁻¹) | Yield (%) |
|---------------|--------------|--------------|---|-----------|
| Cell extract | 1080 | 260 | 0.2 | 100 |
| His GraviTrap | 45 | 244 | 5 | 94 |
| Mono-Q | 12 | 225 | 19 | 87 |
| His GraviTrap | 5 | 170 | 34 | 66 |

TABLE 4 | Crystallographic data collection and refinement statistics of *Rj3HB6H*.

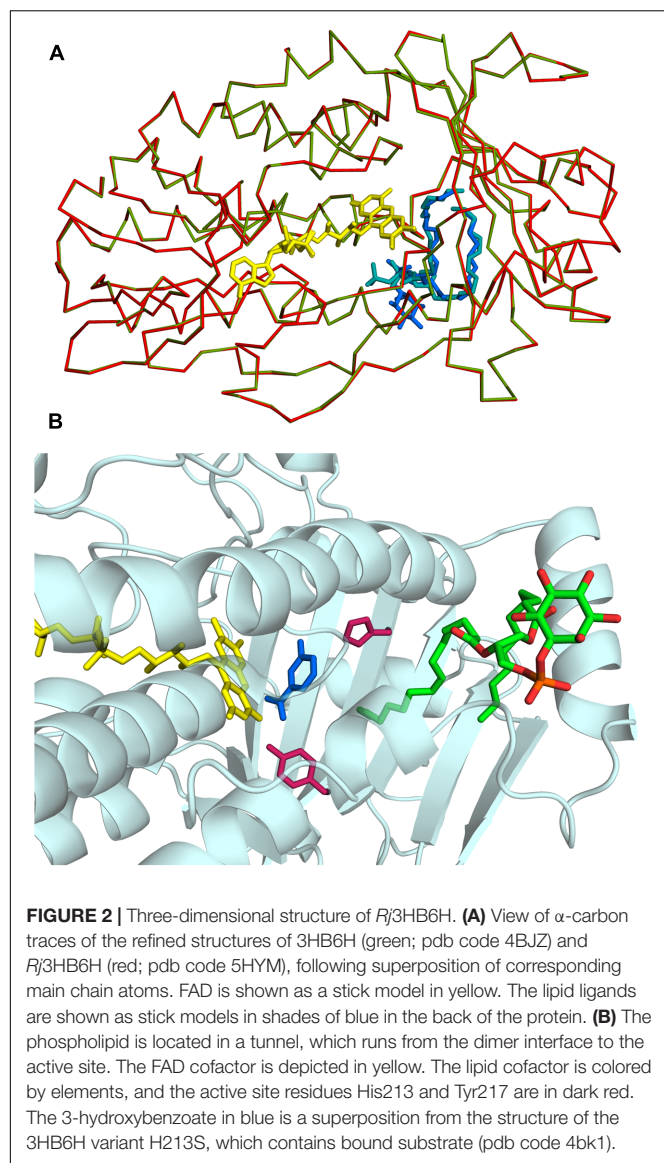
| Protein Data Bank Code | 5HYM |
|-----------------------------------|-------------------------------------|
| Unit cell (Å) | $a = b = 106.98 \text{ c} = 143.39$ |
| Space group | $I4_122$ |
| Resolution (Å) | 2.30 |
| $R_{\text{sym}}^{\text{a,b}}$ (%) | 15.1 (50) |
| Completeness ^b (%) | 99.7 (100) |
| Unique reflections | 18,766 |
| Redundancy ^b | 7.5 (5.8) |
| I/σ^{b} | 8.4 (3.0) |
| No. of atoms | 3,198 |
| Average B value (Å ²) | 33.4 |
| $R_{\text{cryst}}^{\text{c}}$ (%) | 20.6 |
| $R_{\text{free}}^{\text{c}}$ (%) | 26.2 |
| r.m.s. bond length (Å) | 0.015 |
| r.m.s. bond angles (°) | 1.75 |

^a $R_{\text{sym}} = \sum |I_i - \bar{I}| / \sum I_i$ where I_i is the intensity of *i*th observation and \bar{I} is the mean intensity of the reflection. ^bValues in parentheses are for reflections in the highest resolution shell. ^c $R_{\text{cryst}} = \sum |F_{\text{obs}} - F_{\text{calc}}| / \sum F_{\text{obs}}$ where F_{obs} and F_{calc} are the observed and calculated structure factor amplitudes, respectively. R_{cryst} and R_{free} were calculated using the working and test set, respectively. r.m.s., root mean square

lithium sulfate was present instead of sodium acetate. The three-dimensional structure of *Rj3HB6H* was solved at 2.3 Å resolution by molecular replacement (Table 4). The isalloxazine moiety of FAD was refined with full occupancy in the *in* conformation. Similar to the crystallographic analysis of 3HB6H, no substrate could be detected in the active site of the enzyme, despite presence of excess 3-hydroxybenzoate in the crystallization drop. The protein crystallizes as a dimer, just as 3HB6H (Montersino et al., 2013), and contains a phospholipid molecule in each subunit. The electron density of the phospholipid in the crystal structure was refined as two acyl chains, one of twelve and one of seventeen carbon units. Superimposition of the *Rj3HB6H* and 3HB6H models (root mean square deviation = 0.22 Å) shows minor deviations (Figure 2A). The phospholipid is located in a tunnel, which runs from the dimer interface to the active site (Figure 2B), and interacts with the opposite monomer. The phosphate group resides at the protein surface near Arg350 and Lys385, and the electron density of the headgroup is consistent with the presence of a cyclohexanehexol moiety (Figure 3A).

Identification of Protein-Bound Lipid Molecules

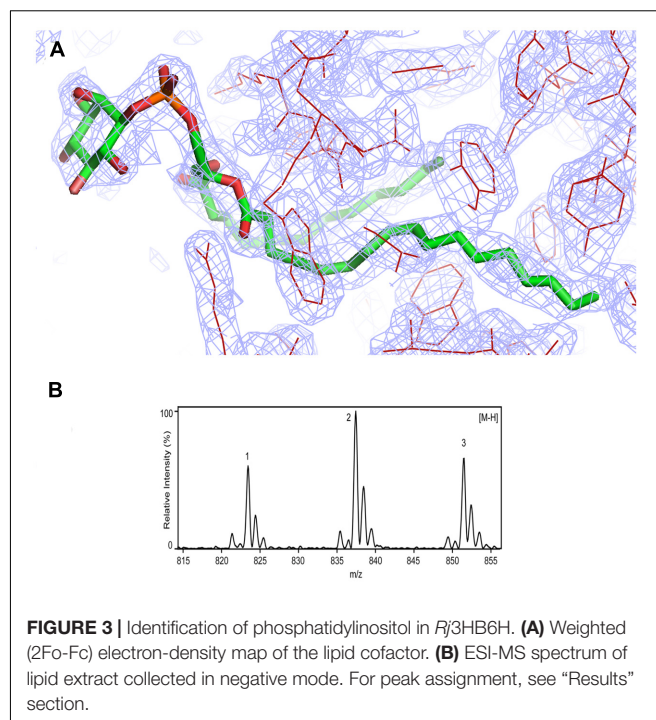
Assignment of protein-bound phospholipids was achieved by ESI-MS analysis of the low molecular weight components



extracted from denatured *Rj3HB6H*. The mass spectrum in negative mode (**Figure 3B**) displayed three main peaks with m/z values of 823, 837, and 851. From the MS pattern it was evident that *Rj3HB6H* binds a phospholipid with a bigger headgroup compared to that of the lipid found in 3HB6H.

Fragmentation analysis and comparison of data to reference lipid MS spectra led to a match of the obtained mass peaks with those of PI, having aliphatic chains containing 15 to 19 carbons. Peak 1 (m/z 823) is assigned to PI (15:0/18:0), peak 2 (m/z 837) is assigned to PI (16:0/18:0) (Sharp et al., 2007; Morita et al., 2011) and peak 3 (m/z 851) is assigned to PI (16:0/19:0) with alternate acylate form (tuberculostearic acid) (Drage et al., 2010).

Typical fragmentation of PI was visible in the MS/MS spectra by signature peaks with m/z values of 153, 223, 241, and 297, representing glycerol phosphate water (m/z 153) and inositol



headgroup fragments (Lang and Philp, 1998; Pulfer and Murphy, 2003; Oursel et al., 2007) (data not shown). Minor peaks at approximately 2 m/z values lower than the identified peaks represent the same PI, containing one unsaturated bond.

Protein Oligomeric Composition

To gain further insight into the enzyme–lipid interaction, we determined the oligomeric protein composition of 3HB6H and *Rj3HB6H* using native MS (Leney and Heck, 2017). As a first step, we determined the experimental masses of the denatured proteins. The measured values ($46,766 \pm 4$ Da for 3HB6H and $46,761 \pm 2$ Da for *Rj3HB6H*) agree with the mass deduced from the primary sequence, lacking the N-terminal methionine.

Native MS of 3HB6H showed eight charge states corresponding to five different protein forms (**Figure 4A** and **Table 5**). The charge state distribution ions +12, +13, and +14 represent the monomeric apoprotein (average mass $46,835 \pm 5$ Da; red stars), the monomeric holoprotein (average mass $47,603 \pm 6$ Da; green stars), and the monomeric holoprotein containing additionally one PG/PE molecule (average mass $48,312 \pm 7$ Da; blue stars). The charge state distribution ions +18, +19, +20, +21, and +22 predominantly represent the dimeric holoprotein with either one or two PG/PE molecules bound (average mass $95,868 \pm 16$ Da; orange stars, and $96,643 \pm 14$ Da; purple stars, respectively). Tandem MS experiments revealed that one, two, three, or four ligands can be expelled from 3HB6H. The assignment of bound ligands was made on the basis of total mass increase and comparison with the mass of the native apoprotein (**Table 5**).

Native MS of *Rj3HB6H* also showed a range of charge state distributions (**Figure 4B** and **Table 5**). The charge state

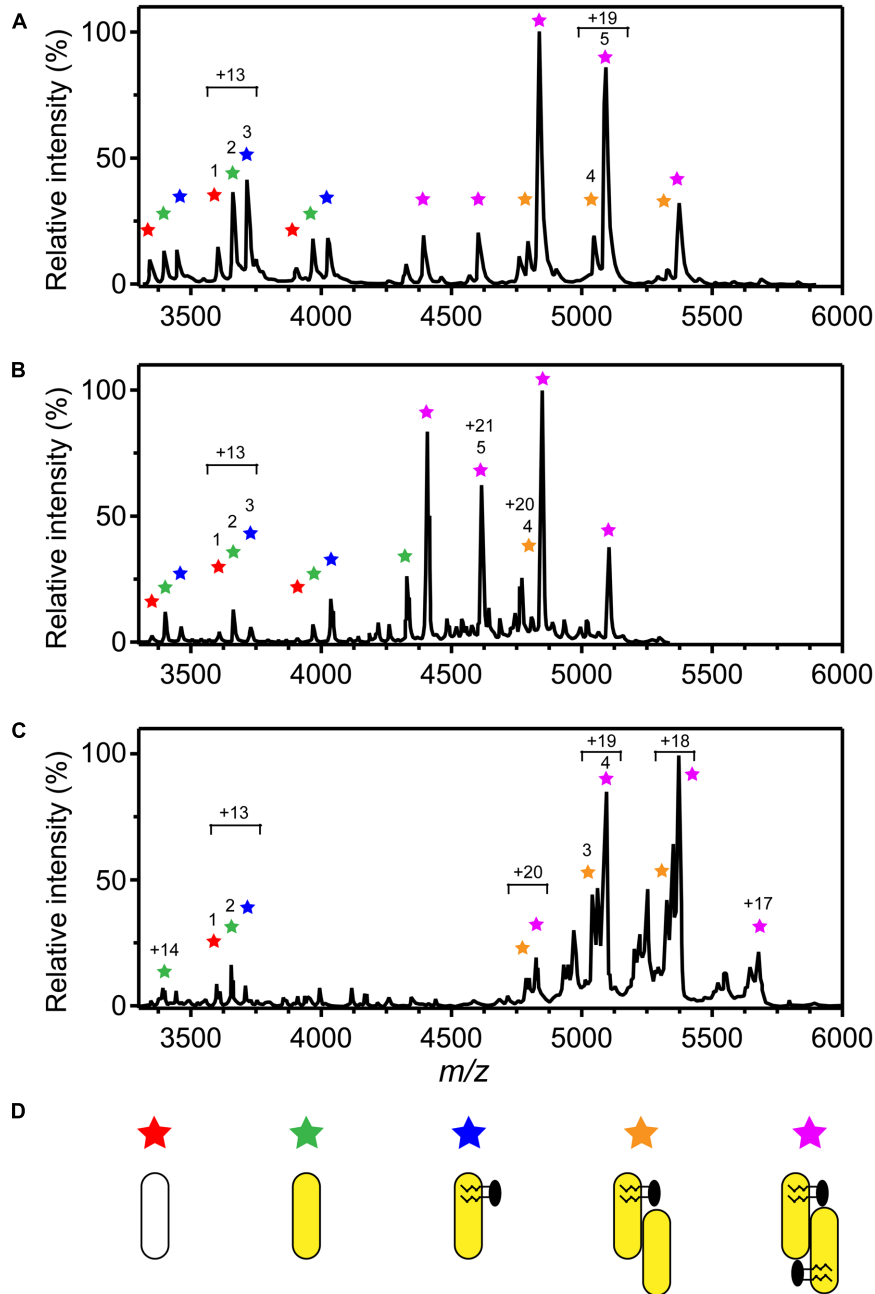


FIGURE 4 | Oligomer distribution and lipid composition of 3HB6H enzymes as determined by native ESI-MS. Mass spectra were recorded in 50 mM ammonium acetate, pH 6.8. **(A)** Mass spectrum of 3HB6H. **(B)** Mass spectrum of *Rj*3HB6H. **(C)** Mass spectrum of *Pa*3HB6H. Masses and intensities of numbered peaks are listed in **Table 5**. **(D)** Cartoons of the various subunit compositions. Apoprotein is indicated in white, holoprotein in yellow and lipid molecules in black.

distribution ions +12, +13, and +14 represent the monomeric apoprotein (average mass $46,829 \pm 1$ Da; red star), the monomeric holoprotein (average mass $47,613 \pm 1$ Da; green stars), and the monomeric holoprotein containing one PI molecule (average mass $48,458 \pm 2$ Da; blue star). The latter species differs from the related 3HB6H species (**Figure 4A**, blue stars) because it has a bigger lipid headgroup. The major species

in the native mass spectrum of *Rj*3HB6H corresponds to the holo-*Rj*3HB6H dimer with PI bound to both subunits (average mass $96,938 \pm 32$ Da; **Figure 4B**, yellow stars). Only by magnification it is possible to detect a minor peak representing the holo-*Rj*3HB6H dimer with one PI bound (average mass $96,128 \pm 5$ Da; **Figure 4B**, orange stars). A cartoon of the different subunit compositions of 3HB6H is presented in **Figure 4D**.

TABLE 5 | Oligomeric forms of 3HB6H determined by native ESI-MS.

| Peak ^a | <i>m/z</i> | Average mass (Da) | Δ mass (Da) |
|-------------------|------------|-------------------|--------------------|
| 3HB6H | | | |
| 1 | 3,603 | 46,835 ± 5 | |
| 2 | 3,663 | 47,603 ± 6 | 767 ^b |
| 3 | 3,717 | 48,312 ± 7 | 1,477 ^b |
| 4 | 5,048 | 95,868 ± 16 | 2,198 ^c |
| 5 | 5,088 | 96,643 ± 14 | 2,973 ^c |
| Rj3HB6H | | | |
| 1 | 3,608 | 46,829 ± 1 | |
| 2 | 3,663 | 47,613 ± 1 | 784 ^b |
| 3 | 3,728 | 48,458 ± 2 | 1,629 ^b |
| 4 | 4,807 | 96,128 ± 5 | 2,470 ^c |
| 5 | 4,616 | 96,938 ± 32 | 3,280 ^c |
| Pa3HB6H | | | |
| 1 | 3,651 | 47,448 ± 2 | 790 ^b |
| 2 | 3,706 | 48,167 ± 2 | 1,509 ^b |
| 3 | 5,035 | 95,662 ± 7 | 2,346 ^c |
| 4 | 5,073 | 96,738 ± 8 | 3,062 ^c |

^aPeaks are indicated in **Figure 4**. ^bCalculated using apo-monomer. ^cCalculated using apo-dimer.

Conservation of Lipid Binding Site

To analyze whether the lipid-binding site of 3HB6H is conserved among species, we explored the natural diversity of 3HB6H enzymes. 3HB6H activity has been reported for Gram-positive and Gram-negative bacteria and for yeasts. Besides from the *R. jostii* prototype, the enzymes from *Klebsiella pneumonia* M5a1 (Suárez et al., 1995; Liu et al., 2005), *Pseudomonas alcaligenes* NCIMB 9867 (Gao et al., 2005), *Polaromonas naphthalenivorans* CJ2 (Park et al., 2007), *Corynebacterium glutamicum* ATCC 12032 (Yang et al., 2010), *Rhodococcus sp.* NCIMB 12038 (Liu et al., 2011) and *Candida parapsilosis* (Holesova et al., 2011) have been characterized to some extent.

From the structural data of the *R. jostii* 3HB6H enzyme and the multiple sequence alignment presented in **Figure 5** it can be inferred that residues directly involved in lipid binding in *Rj3HB6H* are not always conserved in the orthologs; among the bacterial enzymes studied, most sequence divergence occurs in 3HB6H from *P. alcaligenes* NCIMB 9867 (*Pa3HB6H*). This prompted us to study the lipid binding properties of the *Pseudomonas* 3HB6H enzyme.

Expression of the *Pa3HB6H* gene in *E. coli* TOP10 cells yielded about 10 mg of enzyme from a 1 L batch culture. Purified *Pa3HB6H* had a specific activity of 34 U·mg⁻¹ (**Table 3B**) and migrated in SDS-PAGE as a single band with an apparent subunit mass of 47 kDa (not shown). ESI-MS established that native *Pa3HB6H* is a dimer, and not a trimer as suggested earlier (Gao et al., 2005), and that the enzyme indeed contains lipids (**Figure 4C** and **Table 5**). The mass spectrum of extracted lipids showed peaks with *m/z* values characteristic of PG and PE with aliphatic chains ranging from 14 to 19 carbons, similar to the previously identified lipids in 3HB6H from *R. jostii* RHA1 produced in *E. coli* (Monterisino et al., 2013).

DISCUSSION

3HB6H is a flavoenzyme that catalyzes the *para*-hydroxylation of 3-hydroxybenzoate to gentisate, a key step in the catabolism of lignin-derived aromatic compounds in the soil (Pérez-Pantoja et al., 2010). Up to now, 3HB6H is the only flavoprotein monooxygenase that has been found to bind phospholipids (Monterisino et al., 2013). Structural analysis showed that the hydrophobic tails of the phospholipids deeply penetrate into the substrate-binding domains, whereas the hydrophilic parts are exposed on the protein surface, connecting the dimerization domains (**Figure 1**). Attempts to obtain native lipid-free protein were not successful, indicating that the phospholipids are important to attain a properly folded protein (Monterisino et al., 2013).

3HB6H binds a mixture of PG and PE, the major constituents of the *E. coli* inner membrane (Monterisino et al., 2013). By expressing its gene in *R. jostii* RHA1#2, we aimed at unraveling the lipid binding abilities of 3HB6H in the original host. Although *E. coli* gives considerable higher yields (Monterisino and van Berkel, 2012), significant quantities of soluble His-tagged *Rj3HB6H* were obtained. The difference in enzyme yield could be linked to the type of induction and promoter strength used in the *R. jostii* RHA1#2 strain, which is based on the propane monooxygenase operon (Sharp et al., 2007). Nevertheless, our results show that the newly developed *R. jostii* RHA1#2 strain opens new prospects for actinomycetes as host cells for production of recombinant proteins (Nakashima et al., 2005).

Rj3HB6H displayed similar catalytic and structural properties as 3HB6H, and the mode of lipid binding was highly conserved (**Figure 2**). Gratifyingly, the crystallographic data and mass spectrometry analysis provided clear evidence that *Rj3HB6H* contains PI as natural glycerophospholipid cofactor (**Figure 3**). The crystal structure showed that the inositol headgroups of the phospholipids are located at the protein surface, and that the *sn*-2 acyl moieties are in contact with helix 11 of the other subunit (**Figure 1**). Based on MS/MS analysis, we identified the bound phospholipids as a mixture of PIs with carbon chains between 15 and 19 carbons. One of the extracted lipids was identified as tuberculostearic acid, an alternative acylated form of palmitate present in the membranes of *Rhodococcus* and *Mycobacterium* (Drage et al., 2010).

Rj3HB6H is a dimer both in solution and in crystal form, but native MS showed a ratio of monomer to dimer of about 1:3 (**Figure 4B**). Release of only one PI from the dimer resulted in monomerization in the gas phase. A similar observation was made with 3HB6H, but with this enzyme more dimers containing only one bound lipid (PG or PE) were detected (**Figure 4A**). 3HB6H dimers containing two phospholipids seem to be more stable in the gas phase than dimers containing one phospholipid. This strongly supports that lipid binding near the dimer interface stabilizes monomer contacts.

Native MS-analysis showed that *Pa3HB6H* is a homodimer and not a trimer as postulated earlier (Gao et al., 2005). The dimeric nature is in agreement with the structural properties of 3HB6H and *Rj3HB6H*. MS-analysis also revealed that

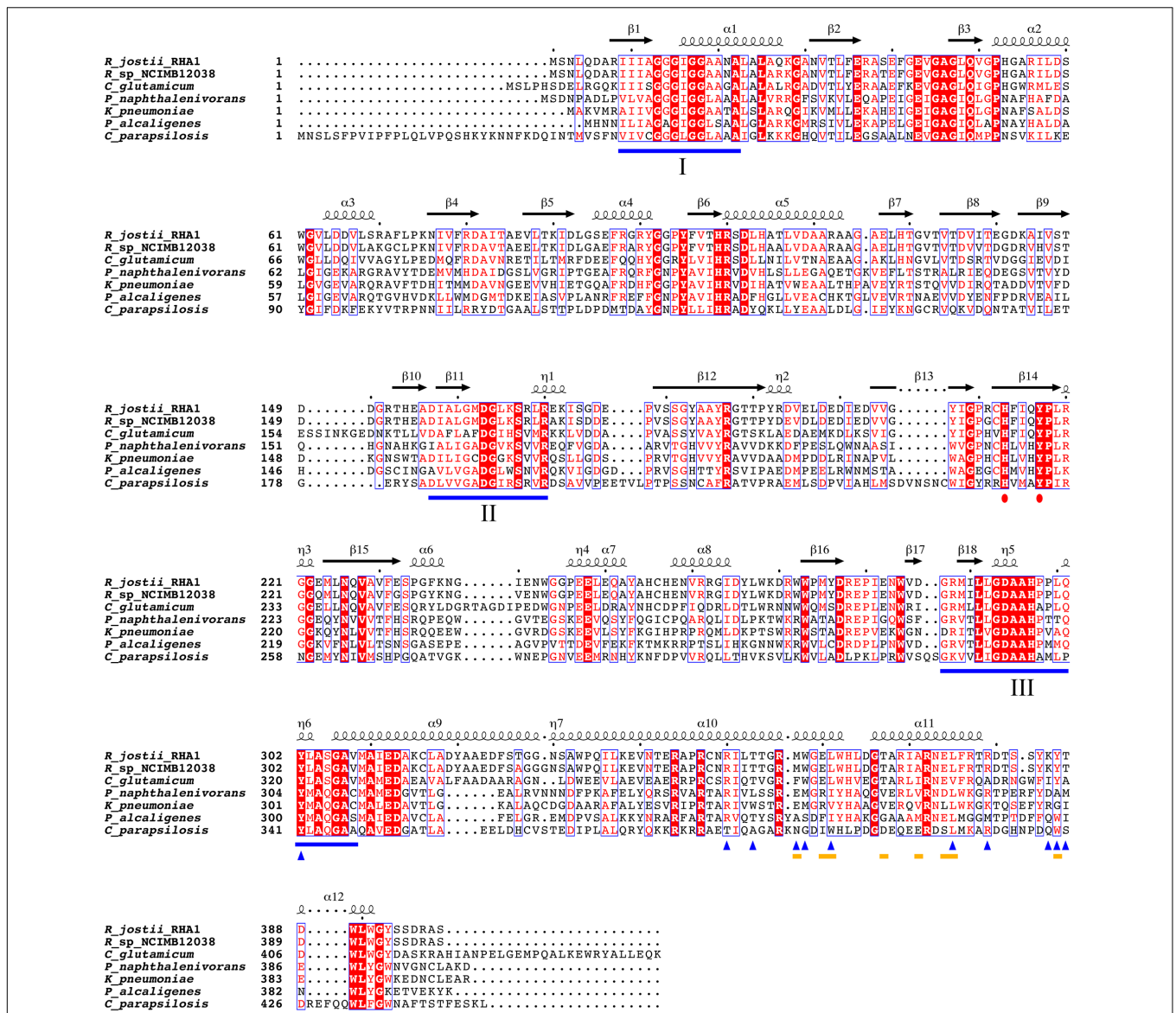


FIGURE 5 | Multiple sequence alignment of known 3HB6H enzymes. UniProt ID numbers: Q05FK6, *R. jostii* RHA1; E7CYP8, *Rhodococcus* sp. NCIMB 12038; Q8NLB6, *C. glutamicum* ATCC 12032; Q3S4B7, *P. naphthalenivorans* CJ2; Q6EXK1, *K. pneumoniae* M5a1; Q9F131, *P. alcaligenes* NCIMB 9867; CPAG_03410, *C. parapsilosis*. Identical residues are shown in red. Flavin binding motifs are underlined in blue [I: GXGXXG; II: DG; III: GD (Eppink et al., 1997)]. The His-Tyr pair involved in substrate binding and hydroxylation is marked with red dots. The yellow lines mark residues involved in dimerization. Blue triangles indicate residues involved in lipid binding. Secondary structure assigned from the 3HB6H crystal structure (4BK1). Diagram was produced using ESPript (Robert and Gouet, 2014).

recombinant *Pa*3HB6H binds the same type of phospholipids as 3HB6H. This supports that lipid binding is an intrinsic property of 3HB6Hs. As a main result, it appears that the 3HB6H family uses phospholipids as a common tool to increase their dimerization strength. Phospholipid binding is independent of the type of lipid headgroup, but relies on the presence of hydrophobic tunnels running from the protein surface to the active site.

Like PG/PE in *E. coli* (Oursel et al., 2007), PI is the major lipid membrane component in *Rhodococcus* (Nigou et al., 2003). This

may explain why PG/PE are found as lipid ligands of 3HB6H and *Pa*3HB6H, while PI is found in *Rj*3HB6H. PI is the precursor for lipoarabinomannan and PI-mannoside synthesis. Glycolipid synthesis and reorganization of membrane composition allow *Rhodococcus* to adapt to environmental changes (Lang and Philp, 1998; Sharp et al., 2007; Guerin et al., 2010; Morita et al., 2011; De Carvalho et al., 2014). Binding of PI may localize 3HB6H at the cytoplasmic membrane, via inositol recognition of other proteins or specific phospholipid patching on the inner side of the membrane (Morita et al., 2011). At those specific spots,

uptake of aromatic compounds from the environment may be coupled more efficiently to their catabolism.

Taking together, phospholipids do not have a direct catalytic role in 3HB6H, but are involved in stabilizing the dimer contact and, possibly, substrate orientation (Montersino et al., 2013). At this stage, we cannot exclude that bound phospholipids have some other function, for instance in directing the cytoplasmic membrane localization or in guiding/protecting molecules from entering the active site. In addition, the *R. jostii* RHA1#2 expression strain described here represents a useful alternative for the production of (whole-cell) biocatalysts.

AUTHOR CONTRIBUTIONS

WvB and LD initiated the project; SM, EtP, AW, AB, AH, RvG, LD, AM, and WvB designed experiments and analyzed data; EtP constructed *Rhodococcus* expression vector Q2+; RO crystallized Rj3HB6H and determined the crystal structure; SM, AW, and AB

performed analytical and biochemical experiments; SM, EtP, AM, AW, and WvB wrote the manuscript.

FUNDING

This study was supported by the Integrated Biosynthesis Organic Synthesis program (IBOS; project number 053.63.013) of the Netherlands Organization for Scientific Research (NWO). Additional support from Proteins At Work (project 184.032.201), a program of the Netherlands Proteomics Centre financed by the Netherlands Organization for Scientific Research (NWO) as part of the National Roadmap Large-scale Research Facilities of the Netherlands is acknowledged.

ACKNOWLEDGMENT

Part of the content of this manuscript has been published in the Ph.D. thesis of Dr. Stefania Montersino (Montersino, 2012).

REFERENCES

- Adams, P. D., Afonine, P. V., Bunkóczy, G., Chen, V. B., Davis, I. W., Echols, N., et al. (2010). PHENIX: a comprehensive Python-based system for macromolecular structure solution. *Acta Crystallogr. D Biol.* 66(Pt 2), 213–221. doi: 10.1107/s0907444909052925
- Brennan, P. J., and Nikaido, H. (1995). The envelope of mycobacteria. *Annu. Rev. Biochem.* 64, 29–63. doi: 10.1146/Annurev.Bi.64.070195.000333
- Chun, J., Kang, S. O., Hah, Y. C., and Goodfellow, M. (1996). Phylogeny of mycolic acid-containing actinomycetes. *J. Ind. Microbiol.* 17, 205–213. doi: 10.1007/Bf01574694
- De Carvalho, C. C., Costa, S. S., Fernandes, P., Couto, I., and Viveiros, M. (2014). Membrane transport systems and the biodegradation potential and pathogenicity of genus *Rhodococcus*. *Front. Physiol.* 5:133. doi: 10.3389/fphys.2014.00133
- Drage, M. G., Tsai, H. C., Pecora, N. D., Cheng, T. Y., Arida, A. R., Shukla, S., et al. (2010). *Mycobacterium tuberculosis* lipoprotein LprG (Rv1411c) binds triacylated glycolipid agonists of Toll-like receptor 2. *Nat. Struct. Mol. Biol.* 17, 1088–1095. doi: 10.1038/nsmb.1869
- Emsley, P., Lohkamp, B., Scott, W. G., and Cowtan, K. (2010). Features and development of Coot. *Acta Crystallogr. D Biol.* 66, 486–501. doi: 10.1107/S0907444910007493
- Eppink, M., Schreuder, H., and van Berkel, W. (1997). Identification of a novel conserved sequence motif in flavoprotein hydroxylases with a putative dual function in FAD/NAD(P)H binding. *Protein Sci.* 6, 2454–2458. doi: 10.1002/pro.5560061119
- Finnerty, W. R. (1992). The biology and genetics of the genus *Rhodococcus*. *Annu. Rev. Microbiol.* 46, 193–218. doi: 10.1146/Annurev.Micro.46.1.193
- Gao, X. L., Tan, C. L., Yeo, C. C., and Poh, C. L. (2005). Molecular and biochemical characterization of the *xlnD*-encoded 3-hydroxybenzoate 6-hydroxylase involved in the degradation of 2,5-xyleneol via the gentisate pathway in *Pseudomonas alcaligenes* NCIMB 9867. *J. Bacteriol.* 187, 7696–7702. doi: 10.1128/JB.187.22.7696-7702.2005
- Guerin, M. E., Korduláková, J., Alzari, P. M., Brennan, P. J., and Jackson, M. (2010). Molecular basis of phosphatidyl-myo-inositol mannoside biosynthesis and regulation in mycobacteria. *J. Biol. Chem.* 285, 33577–33583. doi: 10.1074/jbc.R110.168328
- Gürtler, V., Mayall, B. C., and Seviour, R. (2004). Can whole genome analysis refine the taxonomy of the genus *Rhodococcus*? *FEMS Microbiol. Rev.* 28, 377–403. doi: 10.1016/j.femsre.2004.01.001
- Holesova, Z., Jakubkova, M., Zavadiakova, I., Zeman, I., Tomaska, L., and Nosek, J. (2011). Gentisate and 3-oxoadipate pathways in the yeast *Candida parapsilosis*: identification and functional analysis of the genes coding for 3-hydroxybenzoate 6-hydroxylase and 4-hydroxybenzoate 1-hydroxylase. *Microbiology* 157, 2152–2163. doi: 10.1099/mic.0.048215-0
- Huijbers, M. M. E., Montersino, S., Westphal, A. H., Tischler, D., and van Berkel, W. J. H. (2014). Flavin dependent monooxygenases. *Arch. Biochem. Biophys.* 544, 2–17. doi: 10.1016/j.abb.2013.12.005
- Lang, S., and Philp, J. C. (1998). Surface-active lipids in rhodococci. *Antonie van Leeuwenhoek* 74, 59–70. doi: 10.1023/A:1001799711799
- Leney, A. C., and Heck, A. J. R. (2017). Native mass spectrometry: what is in the name? *J. Am. Soc. Mass Spectrom.* 28, 5–13. doi: 10.1007/s13361-016-1545-3
- Liu, D. Q., Liu, H., Gao, X. L., Leak, D. J., and Zhou, N. Y. (2005). Arg(169) is essential for catalytic activity of 3-hydroxybenzoate 6-hydroxylase from *Klebsiella pneumoniae* M5a1. *Microbiol. Res.* 160, 53–59. doi: 10.1016/j.micres.2004.09.003
- Liu, T. T., Xu, Y., Liu, H., Luo, S., Yin, Y. J., Liu, S. J., et al. (2011). Functional characterization of a gene cluster involved in gentisate catabolism in *Rhodococcus* sp. strain NCIMB 12038. *Appl. Microbiol. Biotechnol.* 90, 671–678. doi: 10.1007/s00253-010-3033-1
- McLeod, M. P., Warren, R. L., Hsiao, W. W. L., Araki, N., Myhre, M., Fernandes, C., et al. (2006). The complete genome of *Rhodococcus* sp RHA1 provides insights into a catabolic powerhouse. *Proc. Natl. Acad. Sci. U.S.A.* 103, 15582–15587. doi: 10.1073/pnas.0607048103
- Montersino, S. (2012). *Structural and Biochemical Characterization of 3-Hydroxybenzoate 6-Hydroxylase*. Doctoral thesis, Wageningen University, Wageningen.
- Montersino, S., Orru, R., Barendregt, A., Westphal, A. H., van Duijn, E., Mattevi, A., et al. (2013). Crystal structure of 3-hydroxybenzoate 6-hydroxylase uncovers lipid-assisted flavoprotein strategy for regioselective aromatic hydroxylation. *J. Biol. Chem.* 288, 26235–26245. doi: 10.1074/jbc.M113.479303
- Montersino, S., Tischler, D., Gassner, G. T., and van Berkel, W. J. H. (2011). Catalytic and structural features of flavoprotein hydroxylases and epoxidases. *Adv. Synth. Catal.* 353, 2301–2319. doi: 10.1002/adsc.201100384
- Montersino, S., and van Berkel, W. J. H. (2012). Functional annotation and characterization of 3-hydroxybenzoate 6-hydroxylase from *Rhodococcus jostii* RHA1. *Biochim. Biophys. Acta* 1824, 433–442. doi: 10.1016/j.bbapap.2011.12.003
- Morita, Y. S., Fukuda, T., Sena, C. B. C., Yamaryo-Botte, Y., McConville, M. J., and Kinoshita, T. (2011). Inositol lipid metabolism in mycobacteria: biosynthesis and regulatory mechanisms. *Biochim. Biophys. Acta* 1810, 630–641. doi: 10.1016/j.bbagen.2011.03.017
- Nakashima, N., Mitani, Y., and Tamura, T. (2005). Actinomycetes as host cells for production of recombinant proteins. *Microb. Cell Fact.* 4:7. doi: 10.1186/1475-2859-4-7

- Ni, Y., Fernandez-Fueyo, E., Baraibar, A. G., Ullrich, R., Hofrichter, M., Yanase, H., et al. (2016). Peroxygenase-catalyzed oxyfunctionalization reactions promoted by the complete oxidation of methanol. *Angew. Chem. Int. Ed. Engl.* 55, 798–801. doi: 10.1002/anie.201507881
- Nigou, J., Gilleron, M., and Puzo, G. (2003). Lipoarabinomannans: from structure to biosynthesis. *Biochimie* 85, 153–166. doi: 10.1016/S0300-9084(03)00048-8
- Oursel, D., Loutelier-Bourhis, C., Orange, N., Chevalier, S., Norris, V., and Lange, C. M. (2007). Lipid composition of membranes of *Escherichia coli* by liquid chromatography/tandem mass spectrometry using negative electrospray ionization. *Rapid Commun. Mass Spectrom.* 21, 1721–1728. doi: 10.1002/rcm.3013
- Park, M., Jeon, Y., Jang, H. H., Ro, H.-S., Park, W., Madsen, E. L., et al. (2007). Molecular and biochemical characterization of 3-hydroxybenzoate 6-hydroxylase from *Polaromonas naphthalenivorans* CJ2. *Appl. Environ. Microbiol.* 73, 5146–5152. doi: 10.1128/AEM.00782-07
- Pérez-Pantoja, D., González, B., and Pieper, D. H. (2010). “Aerobic Degradation of aromatic hydrocarbons,” in *Handbook of Hydrocarbon and Lipid Microbiology*, ed. K. N. Timmis (Berlin: Springer), 799–837. doi: 10.1007/978-3-540-77587-4_60
- Potterton, L., McNicholas, S., Krissinel, E., Gruber, J., Cowtan, K., Emsley, P., et al. (2004). Developments in the CCP4 molecular-graphics project. *Acta Crystallogr. D Biol.* 60, 2288–2294. doi: 10.1107/S0907444904023716
- Pulfer, M., and Murphy, R. C. (2003). Electrospray mass spectrometry of phospholipids. *Mass Spectrom. Rev.* 22, 332–364. doi: 10.1002/mas.10061
- Robert, X., and Gouet, P. (2014). Deciphering key features in protein structures with the new ENDScript server. *Nucleic Acids Res.* 42, W320–W324. doi: 10.1093/nar/gku316
- Schäfer, A., Tauch, A., Jäger, W., Kalinowski, J., Thierbach, G., and Pühler, A. (1994). Small mobilizable multipurpose cloning vectors derived from the *Escherichia coli* plasmids pK18 and pK19: selection of defined deletions in the chromosome of *Corynebacterium glutamicum*. *Gene* 145, 69–73. doi: 10.1016/0378-1119(94)90324-7
- Schrodinger, L. L. C. (2015). “The PyMOL Molecular Graphics System, Version 1.8”.
- Sharp, J. O., Sales, C. M., LeBlanc, J. C., Liu, J., Wood, T. K., Eltis, L. D., et al. (2007). An inducible propane monooxygenase is responsible for N-nitrosodimethylamine degradation by *Rhodococcus* sp strain RHA1. *Appl. Environ. Microbiol.* 73, 6930–6938. doi: 10.1128/AEM.01697-07
- Suárez, M., Ferrer, E., Garridopertierra, A., and Martín, M. (1995). Purification and characterization of the 3-hydroxybenzoate 6-hydroxylase from *Klebsiella pneumoniae*. *FEMS Microbiol. Lett.* 126, 283–290. doi: 10.1111/J.1574-6968.1995.Tb07431.X
- Sucharitakul, J., Medhanavyn, D., Pakotiprapha, D., van Berkel, W. J., and Chaiyen, P. (2015). Tyr217 and His213 are important for substrate binding and hydroxylation of 3-hydroxybenzoate 6-hydroxylase from *Rhodococcus jostii* RHA1. *FEBS J.* 283, 860–881. doi: 10.1111/febs.13636
- Sucharitakul, J., Tongsook, C., Pakotiprapha, D., van Berkel, W. J. H., and Chaiyen, P. (2013). The reaction kinetics of 3-hydroxybenzoate 6-hydroxylase from *Rhodococcus jostii* RHA1 provide an understanding of the para-hydroxylation enzyme catalytic cycle. *J. Biol. Chem.* 288, 35210–35221. doi: 10.1074/jbc.M113.515205
- Sucharitakul, J., Wongnate, T., Montersino, S., van Berkel, W. J. H., and Chaiyen, P. (2012). Reduction kinetics of 3-hydroxybenzoate 6-hydroxylase from *Rhodococcus jostii* RHA1. *Biochemistry* 51, 4309–4321. doi: 10.1021/bi201823c
- Sun, J. H., Kelemen, G. H., Fernández-Abalos, J. M., and Bibb, M. J. (1999). Green fluorescent protein as a reporter for spatial and temporal gene expression in *Streptomyces coelicolor* A3(2). *Microbiology* 145, 2221–2227. doi: 10.1099/00221287-145-9-2221
- Sutcliffe, I. C. (1998). Cell envelope composition and organisation in the genus *Rhodococcus*. *Antonie van Leeuwenhoek* 74, 49–58. doi: 10.1023/A:1001747726820
- Thompson, J. D., Higgins, D. G., and Gibson, T. J. (1994). Clustal-W - improving the sensitivity of progressive multiple sequence alignment through sequence weighting, position-specific gap penalties and weight matrix choice. *Nucleic Acids Res.* 22, 4673–4680. doi: 10.1093/Nar/22.22.4673
- van der Geize, R., and Dijkhuizen, L. (2004). Harnessing the catabolic diversity of *Rhodococcus* for environmental and biotechnological applications. *Curr. Opin. Microbiol.* 7, 255–261. doi: 10.1016/j.mib.2004.04.001
- van der Geize, R., Hessels, G. I., van Gerwen, R., van der Meijden, R., and Dijkhuizen, L. (2002). Molecular and functional characterization of *kshA* and *kshB*, encoding two components of 3-ketosteroid 1- α -hydroxylase, a class IA monooxygenase, in *Rhodococcus erythropolis* strain SQ1. *Mol. Microbiol.* 45, 1007–1018. doi: 10.1046/j.1365-2958.2002.03069.x
- van der Geize, R., Hessels, G. I., van Gerwen, R., Vrijbloed, J. W., van der Meijden, P., and Dijkhuizen, L. (2000). Targeted disruption of the *kstD* gene encoding a 3-ketosteroid delta(1)-dehydrogenase isoenzyme of *Rhodococcus erythropolis* strain SQ1. *Appl. Environ. Microbiol.* 66, 2029–2036. doi: 10.1128/Aem.66.5.2029-2036.2000
- Winn, M. D., Ballard, C. C., Cowtan, K. D., Dodson, E. J., Emsley, P., Evans, P. R., et al. (2011). Overview of the CCP4 suite and current developments. *Acta Crystallogr. D Biol.* 67, 235–242. doi: 10.1107/S0907444910045749
- Yam, K. C., Geize, R., and Eltis, L. D. (2010). “Catabolism of aromatic compounds and steroids by *Rhodococcus*,” in *Biology of Rhodococcus*, ed. M. H. Alvarez (Berlin: Springer), 133–169.
- Yang, Y. F., Zhang, J. J., Wang, S. H., and Zhou, N. Y. (2010). Purification and characterization of the *ncgl2923*-encoded 3-hydroxybenzoate 6-hydroxylase from *Corynebacterium glutamicum*. *J. Basic Microbiol.* 50, 599–604. doi: 10.1002/jobm.201000053

Conflict of Interest Statement: The authors declare that the research was conducted in the absence of any commercial or financial relationships that could be construed as a potential conflict of interest.

Copyright © 2017 Montersino, te Poele, Orru, Westphal, Barendregt, Heck, van der Geize, Dijkhuizen, Mattevi and van Berkel. This is an open-access article distributed under the terms of the Creative Commons Attribution License (CC BY). The use, distribution or reproduction in other forums is permitted, provided the original author(s) or licensor are credited and that the original publication in this journal is cited, in accordance with accepted academic practice. No use, distribution or reproduction is permitted which does not comply with these terms.